

# Roughness Analysis of Realized Volatility and VIX through Randomized Kolmogorov-Smirnov Distribution

Sergio Bianchi<sup>a</sup>, Daniele Angelini<sup>a</sup>

<sup>a</sup>*MEMOTEF, Sapienza University of Rome, Italy*

---

## Abstract

We introduce a novel distribution-based estimator for the Hurst parameter of log-volatility, leveraging the Kolmogorov–Smirnov statistic to assess the scaling behavior of entire distributions rather than individual moments. To address the temporal dependence of financial volatility, we propose a random permutation procedure that effectively removes serial correlation while preserving marginal distributions, enabling the rigorous application of the KS framework to dependent data. We establish the asymptotic variance of the estimator, useful for inference and confidence interval construction. From a computational standpoint, we show that derivative-free optimization methods, particularly Brent’s method and the Nelder–Mead simplex, achieve substantial efficiency gains relative to grid search while maintaining estimation accuracy. Empirical analysis of the CBOE VIX index and the 5-minute realized volatility of the S&P 500 reveals a statistically significant hierarchy of roughness, with implied volatility smoother than realized volatility. Both measures, however, exhibit Hurst exponents well below one-half, reinforcing the rough volatility paradigm and highlighting the open challenge of disentangling local roughness from long-memory effects in fractional modeling.

*Keywords:* Kolmogorov–Smirnov test, VIX, Realized volatility, Hurst–Hölder exponent

---

## 1. Introduction

For several years now, an extensive strand of empirical research in financial econometrics has documented that measures of asset price variability, whether obtained from returns or realized proxies, display strong persistence: their autocorrelation functions decay slowly over time [18, 6, 17, 3, 7]. This stylized fact motivated the use of volatility models exhibiting long memory, that is, processes with non-integrable autocorrelation functions (see e.g. [31] for a review). A prominent example is the fractional

stochastic volatility (FSV) framework of Comte and Renault [16], where the logarithm of volatility evolves according to a fractional Ornstein–Uhlenbeck dynamic driven by fractional Brownian motion (fBm) with Hurst index  $H > 1/2$ , thereby producing a continuous-time specification with genuine long-range dependence. In the more recent years, driven both by theoretical advances in option pricing and implied volatility asymptotics [2, 20] and by empirical findings on realized volatility dynamics [22], research attention has shifted toward so-called *rough* volatility models. In particular, inspired by the FSV framework of Comte and Renault [16], Gatheral, Jaisson, and Rosenbaum [22] propose the Rough Fractional Stochastic Volatility (RFSV) model, which replaces the long-memory setting  $H > 1/2$  by an fBm with  $H < 1/2$ , thus generating paths that are markedly irregular at high frequencies. Rough models raise subtle conceptual issues, since the self-similarity of fBm entails that local roughness cannot be disentangled from asymptotic dependence properties, meaning that one cannot have  $H < 1/2$  and long-memory, exhibited by the process only when  $H > 1/2$ . Also the common workaround to embed fBm within a stochastic differential equation, for instance the fractional Ornstein–Uhlenbeck process underpinning both FSV and RFSV models, does not solve the problem that the Hurst parameter  $H$  simultaneously dictates path roughness and the asymptotic rate of decay of correlations. Consequently, in the rough regime  $H \in (0, 1/2)$ , the fractional Ornstein–Uhlenbeck specification generates dynamics characterized by short-range dependence and pronounced high-frequency roughness. An attempt to decouple the two effect is made by [9], who introduce a new class of continuous-time models of the stochastic volatility that can simultaneously incorporate roughness and slowly decaying autocorrelations.

The picture outlined above shows how pivotal is the estimation of the parameter  $H$  to identify the most appropriate class of models for describing the dynamics of (log) volatility. A variety of estimation methodologies have been proposed, including Power Spectral Density (PSD) estimation [22], wavelet-based techniques such as Wavelet Leaders and Multiresolution Analysis [1], variational methods based on Quadratic Variation [32, 33, 34], as well as Bayesian and maximum likelihood estimation procedures [10]. More recently, deep learning and machine learning approaches have also been explored as promising tools for estimating the Hurst parameter [8].

Following this strand of research, we propose a novel distribution-based estimator of the self-similarity parameter,  $\hat{H}_0$ , built upon the framework of introduced in [11]. Unlike traditional approaches that rely on scaling relations of second moments, this method leverages the Kolmogorov–Smirnov (KS) statistic to compare entire distribu-

tions of rescaled increments, thereby capturing richer structural information and limiting the impact of some nonlinear biases that affect individual moments based estimators [4]. In its classical formulation, the KS statistic is designed for independent samples. Therefore, to overcome the statistical limitations imposed by the strong temporal dependence typical of financial time series, we introduce a random permutation procedure that removes serial correlation while preserving the marginal distribution of the increments (proof in Proposition 2.5). This methodological innovation, combined with an optimization routine designed to guarantee computational efficiency, enables the valid application of the Kolmogorov–Smirnov test to dependent data, thereby addressing a key limitation of earlier estimation approaches. We also derive the estimator’s variance (Proposition 2.6) to establish its asymptotic properties, thereby enabling confidence interval construction and clarifying its convergence behavior. The dynamic application of the estimator to both the VIX and the 5-minute realized volatility of the S&P 500 provides novel empirical evidence on the relative smoothness of implied versus realized volatility. By connecting integration and conditional expectation operators to the smoothing hierarchy of realized and implied volatilities, Proposition 3.1 along with Remark 3.2 offer a theoretical justification for the above findings, which not only confirm but also extend earlier results indicating that the VIX is substantially smoother than realized volatility [28, 27]. However, we find that both implied and realized volatility exhibit Hurst exponents significantly less than 1/2. This finding confirms the importance of the open problem of disentangling roughness from memory properties in fractional models.

The paper is organized as follows: section 2 recalls some preliminaries and describes the methodology; section 3 examines the relationship existing between the roughness of VIX and realized volatility; section 4 compares several optimization methods of the algorithm based on the method discussed in section 2; section 5 provides and discusses the estimates, while conclusions are presented in section 6.

## 2. Methodology

### 2.1. Preliminaries

This section reviews the fundamental concepts underlying the Hurst parameter estimation method proposed by [11]. Since these are largely established concepts, only the definitions will be provided, without delving into their respective justifications.

**Definition 2.1.** A nontrivial stochastic process  $X = \{X_t\}_{t \geq 0}$ , stochastically continuous at  $t = 0$ , is said to be  $H_0$ -self-similar with  $H_0 > 0$  ( $H_0$ -ss) if for every  $a \in \mathbb{R}^+$  and every

finite set of times  $t_1, \dots, t_k$ ,

$$(X_{at_1}, \dots, X_{at_k}) \stackrel{d}{=} (a^H X_{t_1}, \dots, a^H X_{t_k}). \quad (1)$$

**Remark 2.1.** In general, a stochastic process is of course fully characterized by its finite-dimensional distributions, defined for any finite collection of times  $t_1, \dots, t_n$  as:

$$F_{t_1, \dots, t_n}(x_1, \dots, x_n) = \mathbb{P}(X_{t_1} \leq x_1, \dots, X_{t_n} \leq x_n).$$

Clearly, when observing a single path  $\{\mathbf{x}_t\}_{t=1, \dots, T}$  of a stochastic process  $\{X_t\}$  – which is the case covered by our work –, we are limited in what we can infer about its underlying distributions due to the lack of repeated, independent realizations. To estimate a joint distribution  $F_{t_i, t_j}$  from data, many independent observations of the random vector  $(X_{t_i}, X_{t_j})$  would be required, but a single path provides only one paired observation  $(\mathbf{x}_{t_i}, \mathbf{x}_{t_j})$  for any given pair  $(t_i, t_j)$ . This is statistically insufficient to estimate the entire joint distribution and the best we can do is to construct the empirical marginal distribution. Under the assumption of stationarity, we treat the observations  $\mathbf{x}_1, \dots, \mathbf{x}_T$  as draws from a common distribution and compute the empirical CDF  $\hat{F}(x) = \frac{1}{T} \sum_{t=1}^T \mathbf{1}_{\mathbf{x}_t \leq x}$ , where  $\mathbf{1}$  is the indicator function. This limitation is actually the reason why the random permutation method we will propose allows to test a necessary condition of self-similarity, not self-similarity in itself.

**Remark 2.2.** If a  $H_0$ -ss stochastic process  $\{X_t\}_{t \geq 0}$ , with  $X_0 = 0$  a.s., has stationary increments, the increment process is self-similar with the same parameter ( $H_0$ -sssi):

$$\{X_{t+a} - X_t\}_{t \geq 0} \stackrel{d}{=} \{a^{H_0} (X_{t+1} - X_t)\}_{t \geq 0}, \quad \forall a \in \mathbb{R}^+. \quad (2)$$

Building upon the approach presented in [11], the self-similarity exponent  $H_0$  can be estimated by testing the equality of the distributions in equation (1) (or equation (2)). To accomplish this, the Kolmogorov-Smirnov test may be employed.

In fact, given a compact timescale set  $\mathcal{A} = [\underline{a}, \bar{a}] \subset \mathbb{R}^+$  and denoted by  $\Phi_{X_t}(x)$  the cumulative distribution function of the stationary increment process  $Z_{t,a} := X_{t+a} - X_t$ , for any  $a \in \mathcal{A}$ , equality (2) can be written as

$$\Phi_{Z_{t,a}}(x) := \mathbb{P}(Z_{t,a} < x) \stackrel{\text{using eq. (2)}}{=} \mathbb{P}(a^{H_0} Z_{t,1} < x) = \Phi_{Z_{t,1}}(a^{-H_0} x),$$

$$\Phi_{a^{-H} Z_{t,a}}(x) := \mathbb{P}(a^{-H} Z_{t,a} < x) \stackrel{\text{using eq. (2)}}{=} \mathbb{P}(a^{H_0-H} Z_{t,1} < x) = \Phi_{Z_{t,1}}(a^{H-H_0} x),$$

and

$$\delta_{Z_t}(\Psi_H) = \sup_{x \in \mathbb{R}} \left| \Phi_{Z_{t,1}}(a^{H-H_0} x) - \Phi_{Z_{t,1}}(\bar{a}^{H-H_0} x) \right|, \quad (3)$$

where  $\Psi_H := \{\Phi_{a-H} Z_{t,a}(x), a \in \mathcal{A}, x \in \mathbb{R}\}$  is the set of the distribution functions of  $\{a^{-H} Z_{t,a}\}_{t \geq 0}$  and  $\delta_{Z_t}$  is the diameter of  $\Psi_H$  on the metric space  $(\Psi_H, \varphi)$ , where  $\varphi$  is the distance function induced by the sup-norm  $\|\cdot\|_\infty$  with respect to  $\mathcal{A}$ . It is easy to recognize in (3) the Kolmogorov-Smirnov statistic.

The diameter  $\delta(\Psi_H)$  satisfies the following propositions (see [11] for proofs):

**Proposition 2.1.**  $\{Z_{t,a}\}_{t \geq 0}$  is  $H_0$ -ss if and only if, for any  $\mathcal{A} \subset \mathbb{R}^+$ ,  $\delta_{Z_t}(\Psi_{H_0}) = 0$ .

**Proposition 2.2.** Let  $\{Z_{t,a}\}_{t \geq 0}$  be  $H_0$ -ss. Then  $\delta_{Z_t}(\Psi_H)$  is non-increasing for  $H \leq H_0$  and non-decreasing for  $H \geq H_0$ .

**Proposition 2.3.** Let  $\{Z_{t,a}\}_{t \geq 0}$ ,  $\mathbf{x} \geq 0$  or  $\mathbf{x} \leq 0$ ,  $\{\mathcal{A}_i\}_{i=1,\dots,n}$  be a sequence of timescale sets such that, denoted by  $\underline{a}_i = \min(\mathcal{A}_i)$  and by  $\bar{a}_i = \max(\mathcal{A}_i)$ , it is  $\underline{a}_i \leq \underline{a}_j$  and  $\bar{a}_i \geq \bar{a}_j$  for  $i > j$ . Then, with respect to the sequence  $\{\mathcal{A}_i\}$ ,  $\delta_{Z_t}(\Psi_H)$  is: non-decreasing, if  $H \neq H_0$ , or zero, if  $H = H_0$ .

Denoted by  $X_t$  the log-volatility process and by  $\Psi_H$  the set of rescaled distribution of its increments, the idea is to estimate the self-similarity parameter  $H_0$  by seeking the value of  $H \in (0, 1]$  that minimizes the Kolmogorov-Smirnov statistic  $\delta_{Z_t}(\Psi_H)$  of any pair of rescaled distributions of  $Z_{t,a}$ . In fact, Proposition 2.1 ensures that if  $Z_{t,a}$  is  $H_0$ -ss then  $\delta_{Z_t}(\Psi_H)$  has a unique minimum with respect to  $H \in (0, 1]$ , in correspondence of the value  $H_0$ . Thus,

$$\hat{H}_0 = \arg \min_{H \in (0,1]} \hat{\delta}_{Z_t}(\Psi_H) \quad (4)$$

The methodology above described poses two challenges:

- assessing the statistical significance of the minimum, as the distribution of the Kolmogorov-Smirnov (KS) test holds only when the samples are independent and identically distributed. Therefore, it is necessary to modify the input processes of equation (3) to eliminate their correlation and force the statistic to follow the KS distribution. This task can be achieved by employing some results from random permutations theory which are shortly summarized below.
- evaluate the variance of estimator (4). Clearly, determining the variance is important for constructing confidence intervals and assessing the extent to which the parameter—potentially modeled as time-varying—deviates from the equilibrium value consistent with the market efficiency hypothesis.

## 2.2. Random permutations

Since the power spectrum  $S_Z(\omega)$  of a stationary process  $\{Z_n\}_{n \in \mathbb{Z}}$  is defined as the Fourier transform of its covariance function, the autocovariance function can be obtained as the inverse Fourier transform of its power spectrum, i.e.

$$K_Z(q) = \mathbb{E}[Z_n Z_{n-q}] = \int_{-\pi}^{\pi} e^{iq\omega} S_Z(\omega) d\omega. \quad (5)$$

Applying this to the power spectrum of the fractional Gaussian noise  $Z_{t,a}^H$ ,  $a > 0$ , one has

$$S_{Z^H}(\omega) = 2c_H(1 - \cos \omega) \sum_{j \in \mathbb{Z}} |2\pi j + \omega|^{-1-2H}, \quad \forall \omega \in [-\pi, \pi], \quad (6)$$

with  $c_H = \frac{C^2}{2\pi} \sin(\pi H) \Gamma(2H + 1)$  [15]. The structure of (6) can be disrupted by random permutations: given the random sequence  $Z = \{Z_\ell, \ell \in \mathbb{Z}\}$ , a new sequence  $U = \{U_\ell, \ell \in \mathbb{Z}\}$  is defined such that

$$U_\ell = Z_{\bar{\ell}L + b_{\underline{\ell}}}, \quad \ell = \bar{\ell}L + \underline{\ell}, \quad \bar{\ell} \in \mathbb{Z}, \quad 0 \leq \underline{\ell} \leq L-1, \quad (7)$$

where  $b = (b_0, b_1, \dots, b_{L-1})$  is a random permutation of the vector  $(0, 1, \dots, L-1)$ , uniformly distributed such that  $\mathbb{P}(b) = \frac{1}{L!}$ , with  $\bar{\ell}$  and  $\underline{\ell}$  the quotient and the remainder, respectively, of  $\frac{\ell}{L}$ . Based on Section 4 in [26], [5] prove the following

**Proposition 2.4.** Let  $Z^H = \{Z_{\ell,a}^H, \ell \in \mathbb{Z}, a > 0\}$  be a fractional Gaussian noise. Then, the new sequence  $\tilde{Z}^H = \{Z_{\bar{\ell}L + b_{\underline{\ell}} + \phi, a}^H, \ell \in \mathbb{Z}, a > 0\}$ , with an independent random phase  $\phi$  uniformly distributed on the set of integers  $(0, 1, \dots, L-1)$ , has factorizable covariance in the limit of large permutation length  $L$

$$\lim_{L \rightarrow \infty} K_{\tilde{Z}^H}(q) = \mathbb{E} \left[ Z_{\bar{\ell}L + b_{\underline{\ell}} + \phi, a}^H \right] \mathbb{E} \left[ Z_{\bar{\ell}+qL + b_{\underline{\ell}+q} + \phi, a}^H \right] = 0 \quad (8)$$

for  $q \neq 0$ .

**Remark 2.3.** Given the stationarity of a fractional Gaussian noise (fGn), aside from a multiplicative parameter, we can state that  $S_{Z^H}(\omega)$  is the power spectrum of its auto-correlation function; since random permutation acts only on the order of the elements of a sequence and not on their distribution, the structure of self-similarity is maintained, i.e.

$$\{Z_{i,a}^{H_0}\} \stackrel{d}{=} \{a^{H_0} Z_{i,1}^{H_0}\} \quad \Rightarrow \quad \{Z_{iL + b_{\underline{i}} + \phi, a}^{H_0}\} \stackrel{d}{=} \{a^{H_0} Z_{iL + b_{\underline{i}} + \phi, 1}^{H_0}\}.$$

Proposition 2.4 asserts that, for sufficiently large values of  $L$ , the randomly permuted sequence  $\tilde{Z}^H$  can be regarded as a white noise process. For an fGn this occurs starting

from  $L \sim 100$ , as shown in [5]. The rate at which the power spectrum  $K_{\tilde{Z}^H}(q)$  converges to that of white noise depends on the regularity of the original power spectral density  $S_{Z^H}(\omega)$ . For example, the randomly permuted versions of NRZ-type (Non-Return-to-Zero) and Biphase processes approximate white noise behavior as  $L \geq 500$  [26].

**Remark 2.4.** Random permutation preserves marginal distributions ( $k = 1$  in equation (1)), but generally destroys temporal/joint structure across lags. Therefore, the technique we propose constitutes a necessary condition for self-similarity, since any self-similar process must have marginals that scale consistently. However, it is not sufficient, because self-similarity also requires scaling relations to hold for all higher-dimensional distributions ( $k \geq 2$ ), and random permutations generally destroy those. In general, it holds the following

**Proposition 2.5** (necessity). Let  $X = (X_1, \dots, X_N)$  be a finite sample and  $\pi$  be a permutation of the index set  $\{1, \dots, N\}$ . Define  $Y_i := X_{\pi(i)}$ . If  $Y_t = X_{\pi(t)}$  is  $H_0$ -ss for all  $a \in \mathbb{R}^+$ , then  $\pi$  must satisfy the commutation relation

$$\pi(at) = a\pi(t), \quad (9)$$

for all  $t \geq 0$  and  $a \in \mathbb{R}^+$ .

*Proof.* Let  $X = (X_1, \dots, X_N)$  be a finite sample and  $\pi$  be a permutation of the index set  $\{1, \dots, N\}$ . Defining  $Y_i := X_{\pi(i)}$ ,  $H_0$ -ss of  $Y$  would entail

$$\{Y_{at_1}, \dots, Y_{at_k}\} \stackrel{d}{=} \{a^{H_0}Y_{t_1}, \dots, a^{H_0}Y_{t_k}\}, \quad \forall a > 0, t_1, \dots, t_k.$$

that is

$$\{X_{\pi(at_1)}, \dots, X_{\pi(at_k)}\} \stackrel{d}{=} \{a^{H_0}X_{\pi(t_1)}, \dots, a^{H_0}X_{\pi(t_k)}\}. \quad (10)$$

On the other side, by  $H_0$ -ss of  $X$ , for any choice of indices  $s_j$  we have

$$\{X_{as_1}, \dots, X_{as_k}\} \stackrel{d}{=} \{a^{H_0}X_{s_1}, \dots, a^{H_0}X_{s_k}\}. \quad (11)$$

The right-hand side of (10) already matches the right-hand side of (11) if we take  $s_j = \pi(t_j)$ . Thus, the only way to use (11) to replace the left-hand side of (10) is to require that the permutation  $\pi$  commutes with the scaling map  $S_a : t \mapsto at$ , i.e. at the level of indices

$$X_{\pi(at_j)} = X_{a\pi(t_j)}$$

that is

$$\pi(at) = a\pi(t), \quad \forall t \geq 0.$$

If (9) holds for every  $a$ , one has

$$\{X_{\pi(at_1)}, \dots, X_{\pi(at_k)}\} = \{X_{a\pi(t_1)}, \dots, X_{a\pi(t_k)}\} \stackrel{d}{=} \{a^{H_0}X_{\pi(t_1)}, \dots, a^{H_0}X_{\pi(t_k)}\}$$

and  $Y$  inherits self-similarity.  $\square$

For a finite index set  $\{1, \dots, N\}$  and an integer scaling  $a$ , the set of permutations satisfying (9) is extremely small compared to  $N!$ . For large  $N$ , the probability that a uniform random permutation satisfies the commutation property is essentially zero. In the continuous case the probability is literally zero. Thus a random permutation almost surely destroys the commutation relation and hence self-similarity when this is tested on finite-dimensional distributions with  $k \geq 2$ .

Fortunately, this concern is not applicable to marginal distributions ( $k = 1$ ) of a stationary process, which is the case covered by Proposition 2.4. Since the fractional Gaussian noise of lag  $a$  is distributed as  $N(0, \sigma^2 a^{2H_0})$ , each value has exactly the same marginal law and therefore nothing changes under permutation. This is why the random permutation method used to determine the significance of the KS statistic is valid in the one-dimensional case under the assumption of local stationarity of the process.

### 2.3. Variance of the estimator

Concerning the variance of estimator (4), we prove the following

**Proposition 2.6** (*Variance of  $\hat{H}_0$* ). If process  $Z_t$  has normally distributed increments decorrelated by random permutation, the variance of estimator (3) is

$$Var(\hat{H}_0) \approx \frac{2\pi e}{(\ln a)^2} \left( \frac{1}{\sqrt{n}} + \frac{1}{\sqrt{m}} \right)^2. \quad (12)$$

*Proof.* To calculate the variance of  $\hat{H}_0$  we can first evaluate the sensitivity of  $\delta_{Z_t^{H_0}}(\Psi_H)$  to changes in  $H$ . This because, since the variance of  $\Phi_{Z_{t,1}^{H_0}}$  equals 1, changing  $H$  only affects the variance of the scaled process  $Z_{t,a}^{H_0}$ , which in turn affects the diameter by changing the point  $\bar{a}^{H-H_0}x$ . In general let us denote by  $\Phi(x; v)$  the cumulative distribution function (CDF) of a Gaussian r.v. with mean 0 and variance  $v$ . The problem becomes to analyze how the diameter

$$D(v) = \sup_x |\Phi(x; 1) - \Phi(x; v)| \quad (13)$$

behaves as a function of  $v$ .

First, observe that the maximum absolute difference between the two CDFs theoretically occurs at points  $\pm\sqrt{\frac{\ln v}{1-1/v}}$ , i.e. at the two points of intersection between the corresponding densities. This means that for empirical CDFs the maximum absolute difference occurs somewhere around these points. First, let us approximate the diameter for small deviations in  $v$  from 1. Set  $v = 1 + \epsilon$ , where  $\epsilon$  is small and expand  $\Phi(x; 1 + \epsilon)$  around  $\epsilon = 0$ :

$$\Phi(x; 1 + \epsilon) \approx \Phi(x; 1) + \epsilon \cdot \frac{\partial \Phi}{\partial v}(x; 1). \quad (14)$$

Since  $\Phi$  is Gaussian, the derivative evaluated at  $v = 1$  is

$$\frac{\partial \Phi}{\partial v}(x; 1) = -\frac{xe^{-x^2/2}}{2\sqrt{2\pi}} = -\frac{x}{2}\phi(x), \quad (15)$$

where  $\phi(x)$  denotes the standard normal density. Thus, for small  $\epsilon$ ,

$$\Phi(x; 1 + \epsilon) - \Phi(x; 1) \approx -\frac{\epsilon}{2}x\phi(x) \quad (16)$$

and therefore the absolute difference between CDFs is approximately linear in  $\epsilon$  with coefficient  $-\frac{1}{2}x\phi(x)$ , i.e.

$$D(1 + \epsilon) \approx \sup_x \left| -\frac{\epsilon}{2}x\phi(x) \right| = \frac{|\epsilon|}{2} \sup_x |x\phi(x)|. \quad (17)$$

Function  $x\phi(x)$  is maximized at  $x = \pm 1$ , where it attains  $\phi(\pm 1) = \pm \frac{1}{\sqrt{2\pi}}e^{-1/2}$ . This gives the approximate diameter for small variance perturbations. Since in our case the variance perturbation is not  $\epsilon$  but  $a^{2(H_0 - H)} - 1$ , setting  $v(H) = a^{2(H_0 - H)}$ , for  $H$  close to  $H_0$ , we can write:

$$v(H) = a^{2(H_0 - H)} = e^{2(H_0 - H) \ln a} \approx 1 + 2(H_0 - H) \ln a. \quad (18)$$

Therefore, the perturbation in variance is approximately  $\epsilon = 2(H_0 - H) \ln a$ . Plugging this into (17), one has that the diameter is approximately linear in  $|H - H_0|$  with slope  $|\ln a|/\sqrt{2\pi e}$ . This is the theoretical approximation for the diameter between two Gaussian distribution with variances 1 and  $a^{2(H_0 - H)}$ .

Since we deal with empirical CDFs based on finite samples, the DKW inequality<sup>1</sup> applies, therefore the fluctuations around the theoretical value are of order  $O_p(1/\sqrt{n} + 1/\sqrt{m})$ . In fact, in the two-sample case, to bound the difference between the empirical and theoretical diameter, one can decompose the error using the triangle inequality:

$$\sup_x |F_n(x) - G_m(x)| \leq \underbrace{\sup_x |F_n(x) - F(x)|}_{\text{Error in } F_n} + \underbrace{\sup_x |F(x) - G(x)|}_{\text{Theoretical diameter}} + \underbrace{\sup_x |G(x) - G_m(x)|}_{\text{Error in } G_m}. \quad (19)$$

---

<sup>1</sup>The Dvoretzky–Kiefer–Wolfowitz–Massart inequality (DKWM)

$$P \left( \sup_{x \in \mathbb{R}} |F_n(x) - F(x)| > \epsilon \right) \leq 2e^{-2n\epsilon^2} \quad \text{for any } \epsilon > 0$$

provides a bound on the worst case distance of the empirical distribution function  $F_n(x)$  from its associated population distribution function  $F(x)$ . The inequality, which strengthens the Glivenko–Cantelli theorem by quantifying the rate of convergence as  $n$  tends to infinity, implies that the empirical CDF converges uniformly to the true CDF at a rate  $O_p(1/\sqrt{n})$ . In the two sample-case the DKWM inequality holds for  $m = n \geq 458$ , see [35].

At  $H = H_0$ ,  $\sup_x |F(x) - G(x)| = 0$ , therefore

$$\sup_x |F_n(x) - G_m(x)| \leq \underbrace{\sup_x |F_n(x) - F(x)|}_{\text{Error in } F_n} + \underbrace{\sup_x |G(x) - G_m(x)|}_{\text{Error in } G_m}.$$

$$O_p\left(\frac{1}{\sqrt{n}}\right) + O_p\left(\frac{1}{\sqrt{m}}\right) \quad (20)$$

Thus the total fluctuation is  $O_p\left(\frac{1}{\sqrt{n}} + \frac{1}{\sqrt{m}}\right)$ .

To minimize the empirical KS distance, we balance the bias term  $D\left(a^{2(H_0-H)}\right) \approx |H_0 - H| |\ln a| / \sqrt{2\pi e}$  and the variance term  $O_p(1/\sqrt{n} + 1/\sqrt{m})$ . Setting the bias equal to the standard deviation:

$$|H_0 - H| \frac{|\ln a|}{\sqrt{2\pi e}} \sim \frac{1}{\sqrt{n}} + \frac{1}{\sqrt{m}}. \quad (21)$$

It follows

$$\hat{H}_0 - H_0 \sim \frac{\sqrt{2\pi e}}{|\ln a|} \left( \frac{1}{\sqrt{n}} + \frac{1}{\sqrt{m}} \right) Z, \quad (22)$$

where  $Z \sim N(0, 1)$ . This entails that the asymptotic variance is

$$\text{Var}(\hat{H}_0) \approx \frac{2\pi e}{(\ln a)^2} \cdot \left( \frac{1}{\sqrt{n}} + \frac{1}{\sqrt{m}} \right)^2 \quad (23)$$

and the rate of convergence of  $\hat{H}_0$  to  $H_0$  is  $O_p(1/\sqrt{n} + 1/\sqrt{m})$ .  $\square$

Thus, extracting two rescaled and randomized samples  $Z_{1,\cdot}$  and  $Z_{2,\cdot}$ , of length  $n$  and  $m$  respectively and referred to time scales  $\underline{a}$  and  $\bar{a}$ , with empirical CDFs  $\Phi_{1,n}$  and  $\Phi_{2,m}$ , the empirical diameter is

$$\hat{\delta}_{Z_t}(\Psi_H) = \sup_{x \in \mathbb{R}} |\Phi_{1,n}(x) - \Phi_{2,m}(x)| = \sup_{x \in \mathbb{R}} \left| \frac{1}{n} \sum_{i=1}^n \mathbb{1}_{\underline{a}^{-H} Z_{1,i} \leq x} - \frac{1}{m} \sum_{i=1}^m \mathbb{1}_{\bar{a}^{-H} Z_{2,i} \leq x} \right| \quad (24)$$

and the estimated self-similarity parameter is  $\hat{H}_0 = \arg \min_{H \in (0,1]} \hat{\delta}_{Z_t}(\Psi_H)$ , provided that  $\hat{\delta}_{X_t}(\Psi_H)$  can be considered negligible by comparison with the critical value of the KS test ([5]).

### 3. Roughness of VIX and realized volatility

It is empirically documented in literature (see, e.g., [28, 27]) that the VIX index ( $\text{VIX}_t$  in the following), which serves as a proxy for the market's expectation of future

30-day volatility, has a smoother behavior compared to realized volatility ( $RV_t$  in the following) and to the instantaneous spot volatility ( $\sigma_t$ ). This can be attributed to both theoretical and structural reasons rooted in stochastic modeling. An intuitive explanation of such a difference can be given considering that both realized volatility and VIX are transformations of the spot volatility process.

The realized volatility, square root of

$$RV_t^2 \approx \int_{t-1}^t \sigma_s^2 ds. \quad (25)$$

is a backward-looking average of past volatility computed from intraday returns, capturing actual price fluctuations. The Itô isometry links high-frequency returns to quadratic variation, but market microstructure noise and jumps introduce a  $O_p(n^{-1/2})$  term, lowering  $H$ . The roughness depends on the sampling frequency: being contaminated by bid-ask bounce and price discreteness which induce negative autocorrelation in returns, higher frequencies (e.g., 5-minute intervals) capture more microstructure and short-term noise, leading to very rough estimates ( $H \approx 0.05\text{--}0.15$ ), while lower frequencies (e.g., daily) average out noise and smooth over short-term fluctuations, yielding higher Hurst estimates ( $H \approx 0.15\text{--}0.25$ ).

On the other side, the VIX

$$VIX_t^2 \approx \mathbb{E}_t^{\mathbb{Q}} \left[ \frac{1}{T} \int_t^{t+T} \sigma_s^2 ds \right] \quad (26)$$

is a forward-looking, risk-neutral expectation over a future interval of time and is derived from S&P 500 options prices, reflecting the market's expectation of 30-day volatility. It aggregates information across strikes and maturities, smoothing out high-frequency noise.

Even if the instantaneous volatility  $\sigma_t$  is rough ( $H \approx 0.1$ ), the integral is a bounded linear operator that increases regularity over  $[t, t + \tau]$  (if  $\sigma_t^2$  has Hölder exponent  $H$ , the integral has Hölder exponent  $H + 1$ , reducing roughness). In addition, risk-neutral pricing introduces persistence via volatility risk premiums, further smoothing  $VIX_t$ .

The realized volatility (25) involves a Volterra-type integral operator and it is a

known result from real analysis that if  $f \in C^\alpha$ , then

$$g(t) := \int_t^{t+\Delta} f(s) ds \in C^{\alpha+1}.$$

Therefore, averaging increases Hölder regularity and hence  $H_{\text{realized}} > H_{\text{spot}}$ .

VIX index further involves conditional expectation (26). Therefore, the process involves two distinct smoothing operations: time integration—which, as noted, enhances regularity—and the conditional expectation with respect to a filtration, which further smoothes out irregularities (e.g., through the application of Doob's inequality). Consequently, the hierarchy of roughness exponents emerges:  $H_{\text{VIX}} > H_{\text{realized}} > H_{\text{spot}}$ . This informal explanation finds a rigorous argument in the following

**Proposition 3.1.** Let  $(\Omega, \mathcal{F}, \{\mathcal{F}_t\}_{t \geq 0}, \mathbb{Q})$  be a filtered probability space. Let  $X$  be a r.v. valued in  $[0, \infty)$  such that  $\mathbb{E}(X^2) < \infty$ . Let  $V := \mathbb{E}(X | \mathcal{F}_t)$ , so that  $V$  is  $\mathcal{F}_t$ -measurable,  $V \geq 0$  almost surely, and  $\mathbb{E}(V) = \mathbb{E}(X) < \infty$ . Then:

1.  $\text{Var}(X) \geq \text{Var}(V)$
2.  $\text{Var}(\sqrt{X}) \geq \text{Var}(\sqrt{V})$ .

*Proof.*

1.  $\text{Var}(X) \geq \text{Var}(V)$ .

Since  $X \in L^2$ , the law of total variance holds:

$$\text{Var}(X) = \mathbb{E}[\text{Var}(X | \mathcal{F}_t)] + \text{Var}[\mathbb{E}(X | \mathcal{F}_t)].$$

The term  $\mathbb{E}[\text{Var}(X | \mathcal{F}_t)]$  is nonnegative, hence

$$\text{Var}(X) \geq \text{Var}(V).$$

Equality holds if and only if  $\text{Var}(X | \mathcal{F}_t) = 0$  almost surely, that is, if  $X$  is  $\mathcal{F}_t$ -measurable (equivalently,  $X = V$  almost surely).

2.  $\text{Var}(\sqrt{X}) \geq \text{Var}(\sqrt{V})$ .

Since  $X \geq 0$  and  $\mathbb{E}(X) < \infty$ , we also have  $\sqrt{X} \in L^1$ . Indeed, by Jensen's inequality, the concave function  $x \mapsto \sqrt{x}$  satisfies

$$\mathbb{E}(\sqrt{X}) \leq \sqrt{\mathbb{E}(X)} < \infty,$$

Similarly,  $V \geq 0$  and  $\mathbb{E}(V) = \mathbb{E}(X) < \infty$  imply  $\sqrt{V} \in L^1$  with

$$\mathbb{E}(\sqrt{V}) \leq \sqrt{\mathbb{E}(V)} = \sqrt{\mathbb{E}(X)} < \infty.$$

The variances are:

$$\text{Var}(\sqrt{X}) = \mathbb{E}[(\sqrt{X})^2] - (\mathbb{E}[\sqrt{X}])^2 = \mathbb{E}(X) - [\mathbb{E}(\sqrt{X})]^2,$$

and, since  $\mathbb{E}[V] = \mathbb{E}[X]$ ,

$$\text{Var}(\sqrt{V}) = \mathbb{E}[(\sqrt{V})^2] - [\mathbb{E}(\sqrt{V})]^2 = \mathbb{E}(V) - [\mathbb{E}(\sqrt{V})]^2 = \mathbb{E}(X) - [\mathbb{E}(\sqrt{V})]^2.$$

Subtracting the two expressions we obtain

$$\text{Var}(\sqrt{X}) - \text{Var}(\sqrt{V}) = [\mathbb{E}(\sqrt{V})]^2 - [\mathbb{E}(\sqrt{X})]^2 = [\mathbb{E}(\sqrt{V}) - \mathbb{E}(\sqrt{X})][\mathbb{E}(\sqrt{V}) + \mathbb{E}(\sqrt{X})]. \quad (27)$$

To conclude that the left-hand side is nonnegative it suffices to show that

$$\mathbb{E}(\sqrt{V}) \geq \mathbb{E}(\sqrt{X}).$$

To this aim, observe that the function  $g(x) = \sqrt{x}$  is concave on  $[0, \infty)$ . Applying conditional Jensen's inequality with respect to the  $\sigma$ -algebra  $\mathcal{F}_t$  we obtain (almost surely)

$$\sqrt{\mathbb{E}(X | \mathcal{F}_t)} \geq \mathbb{E}(\sqrt{X} | \mathcal{F}_t).$$

By definition,  $\sqrt{\mathbb{E}(X | \mathcal{F}_t)} = \sqrt{V}$ . Thus, pointwise

$$\sqrt{V} \geq \mathbb{E}(\sqrt{X} | \mathcal{F}_t) \quad (\text{a.s.}). \quad (28)$$

Since  $\sqrt{V} \in L^1$  and that  $\mathbb{E}(\sqrt{X} | \mathcal{F}_t) \in L^1$ , we can take expectations in (28). By monotonicity of expectation we get

$$\mathbb{E}(\sqrt{V}) \geq \mathbb{E}[\mathbb{E}(\sqrt{X} | \mathcal{F}_t)] = \mathbb{E}(\sqrt{X}).$$

From the last inequality and the factorization in (27) it follows that

$$\text{Var}(\sqrt{X}) - \text{Var}(\sqrt{V}) \geq 0,$$

that is,

$$\text{Var}(\sqrt{X}) \geq \text{Var}(\sqrt{V}).$$

□

**Remark 3.1.** If  $\text{Var}(\sqrt{X}) = \text{Var}(\sqrt{V})$ , then necessarily  $\mathbb{E}(\sqrt{V}) = \mathbb{E}(\sqrt{X})$ . By the conditional Jensen inequality (28), if the expectations are equal then  $\sqrt{V} = \mathbb{E}(\sqrt{X} | \mathcal{F}_t)$  almost surely. By the equality condition in Jensen's inequality (for concave functions), this implies that  $\sqrt{X}$  is  $\mathcal{F}_t$ -measurable almost surely, hence  $X$  is  $\mathcal{F}_t$ -measurable

and thus  $X = V$  almost surely (the case in which all variances coincide).

**Remark 3.2** (Roughness of VIX and RV). Proposition 3.1 proves that the variance of realized volatility is larger than the variance of VIX. This result follows from setting  $X := RV_{t,t+T}^2$  and  $\text{VIX}_t^2 = \mathbb{E}^{\mathbb{Q}}[X \mid \mathcal{F}_t]$ . In fact, by construction, the VIX is defined as the risk-neutral conditional expectation of future variance over the next 30 calendar days, annualized:

$$\text{VIX}_t^2 \approx \frac{1}{T} \mathbb{E}^{\mathbb{Q}} \left( \int_t^{t+T} \sigma_s^2 ds \mid \mathcal{F}_t \right), \quad (29)$$

where  $\sigma_s^2$  is the instantaneous variance of the underlying index under the risk-neutral measure  $\mathbb{Q}$ . In practice, this expectation is computed from a strip of out-of-the-money option prices through model-free formulas. Equation (29) indicates that the averaging nature of the VIX operates not only on the variance — which is lower than the variance of realized volatility, as established in Proposition 3.1 — but also on its degree of roughness, which is likewise expected to be smaller than the roughness of the realized volatility, for the same reason (i.e.  $H_{\text{VIX}} > H_{\text{RV}}$ ). This result is in accordance with recent findings in [4, 12], where it is stated that, under mild regularity assumptions given on the large class of stochastic processes known as Multifractional Processes with Random Exponents (MPRE), the conditional variance of a short-lag increment  $h$  satisfies

$$\text{Var}(X_{t+h} - X_t \mid \mathcal{F}_t^{H,\nu}) \sim A(H_t)|h|^{2H_t} \nu_t^2, \quad h \rightarrow 0,$$

with

$$A(H) = \frac{\Gamma(H + \frac{1}{2})^2}{2H \sin(\pi H) \Gamma(2H)}$$

Function  $A(H)$  attains its unique global minimum on  $(0, 1)$  at  $H^* \approx 0.6729$ , which means that the unit lag variance decreases in  $(0, 0.6729)$  as  $H$  increases. In empirical applications of financial interest, the estimated values of  $H$  typically lie within this interval, and it is therefore reasonable to infer an inverse relationship between variance and regularity, as captured by the Hurst–Hölder exponent. This, in turn, supports the conclusion that  $H_{\text{VIX}} > H_{\text{RV}}$ , that is, realized volatility exhibits greater roughness than the VIX.

#### 4. Optimization and Computational Efficiency of the Estimation Method

The estimation of  $H$  can be approached using the methodology described in Section 2. A natural starting point is the Grid Search (GS) procedure, which discretizes the interval  $(0, 1]$  into an equally spaced grid, evaluates the objective function at each grid point, and selects the value of  $H$  that minimizes the Kolmogorov–Smirnov statistic (see Algorithm 1). While GS is straightforward and robust, it rapidly becomes computationally intensive when a fine grid is required. In particular, the computational cost

increases linearly with the number of grid points, rendering the method inefficient for large-scale experiments or repeated estimations.

---

**Algorithm 1** Grid\_Search.exe

---

▷ *Grid Search (GS) method to estimate the  $\hat{H}_0$  that minimizes the KS statistic  $\hat{\delta}_{Z_t}(\Psi_H)$  using the methodology described in the Section 2* ◁

Setting  $\Delta H$  as the grid step, we define a uniform mesh  $H = [H_{start}, 1]$  with  $H_{start} = \Delta H$ .

The set of timescales  $\mathcal{A}$  is completely defined by  $\underline{a} = 1$  and  $\bar{a} > 1$ .

We define the fBm parameters:  $H_0$  is the true Hurst parameter,  $N$  is the length process.

Finally, we define the subsequence length  $T$  for the random method.

▷ *Simulation of the fractional Brownian motion* ◁

Simulation of a fBm  $X^{H_0}$  using the *fbmwoodchan(N,H0)*<sup>2</sup>

Computation of two fGn:  $Z_{\cdot,1}^{H_0}$  and  $Z_{\cdot,\bar{a}}^{H_0}$

▷ *Random permutation of T values from the process Z with function randperm(Z,T) [see prop.2.4]* ◁

Randomization and permutation:  $\tilde{Z}_{\cdot,1}^{H_0} = \text{randperm}(Z_{\cdot,1}^{H_0}, T)$  and  $\tilde{Z}_{\cdot,\bar{a}}^{H_0} = \text{randperm}(Z_{\cdot,\bar{a}}^{H_0}, T)$

▷ *Minimum search* ◁

Initialize  $i$  to 0

**for** all  $H_i$  ranging from  $\Delta H$  to 1 with step size  $\Delta H$  **do**

    Increment  $i$  by 1

    ▷ *Computation of the KS statistic using the function kstest2(·, ·)* ◁

$\hat{\delta}_{\tilde{Z}_\cdot}(\Psi_{H_i}) = \text{kstest2}(\tilde{Z}_{\cdot,1}^{H_0}, \bar{a}^{H_i} \tilde{Z}_{\cdot,\bar{a}}^{H_0})$

    ▷ *Computation of the minimum of the function  $\hat{\delta}_{\tilde{Z}_\cdot}(\Psi_H)$  and the grid step  $i^*$  relative to  $\hat{H}_0$*  ◁

$[\hat{\delta}_{\tilde{Z}_\cdot}(\Psi_{H_0}), i^*] = \min(\hat{\delta}_{\tilde{Z}_\cdot}(\Psi_H))$

$\hat{H}_0 = H_{i^*}$

---

To address these limitations, we evaluate several well-established derivative-free optimization methods: Genetic Algorithm (GA) [23], Simulated Annealing (SA) [25], Particle Swarm (PS) [30], Direct Search (DS) [24], Brent's Method (BM) [14], and Nelder-Mead (NM) [29].

---

<sup>2</sup>The *fbmwoodchan()* is a function based on the Wood and Chan circulating matrix method [36]. In our work we used the MATLAB function available in the FracLab Toolbox 2.02 (INRIA package).

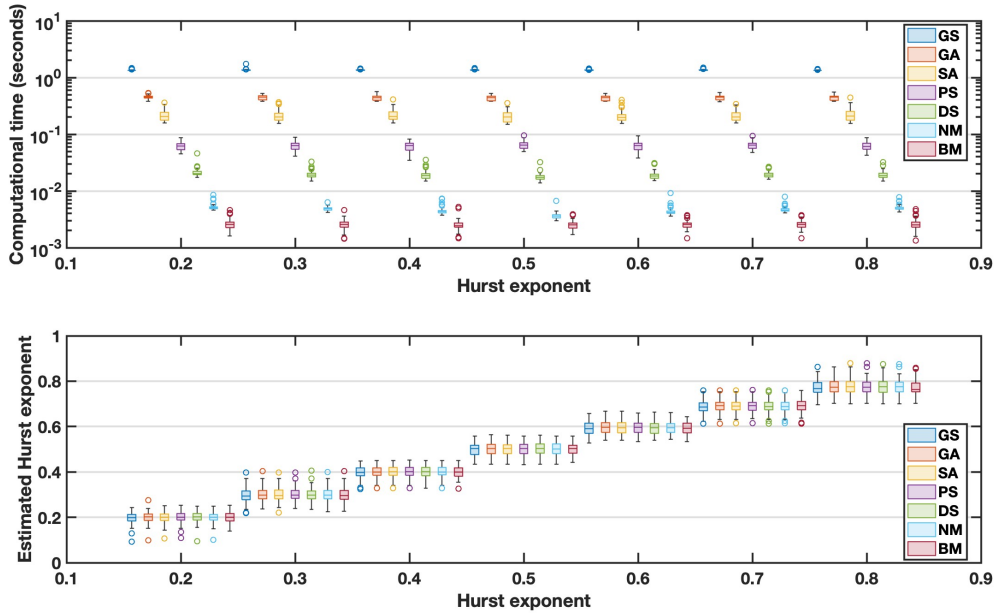


Figure 1: Top panel: Computational time (in seconds) distributions required by the seven optimization methods—Grid Search (GS), Genetic Algorithm (GA), Simulated Annealing (SA), Particle Swarm (PS), Direct Search (DS), Brent’s Method (BM), and Nelder–Mead (NM)—across different values of the Hurst parameter  $H$ . The GS displays markedly higher computational costs due to the discretization step, while derivative-free methods achieve substantially faster convergence. Bottom panel: Empirical distributions of the estimated Hurst parameter obtained with each optimization method, showing that despite differences in computational burden, all routines deliver comparable accuracy. Results are based on 100 simulations.

In the implementation of the GS, we set the grid step to  $\Delta H = 10^{-4}$ , the upper scaling parameter  $\bar{a} = 50$ , the subsequence length  $T = 500$ , the process length  $N = 2^{12}$ . For the alternative optimization methods, instead of discretizing the parameter space, we imposed a tolerance level of  $10^{-6}$ . It is worth noting that, since GS operates on a fixed mesh of abscissae, no direct tolerance criterion was applied to the objective function  $\delta(\Psi_H)$ . Nevertheless, with the chosen parameters, the accuracy around the minimum value of  $\delta(\Psi_H)$  was of the order  $10^{-3}$ . This level is acceptable because it does not alter the location of the estimated Hurst parameter, while guaranteeing numerical stability and keeping the GS computationally feasible for comparison with the other methods.

Figure 1 reports the computational times of the seven optimization methods across different values of the Hurst parameters  $H \in [0.2, 0.8]$  for 100 simulations each. As expected, GS exhibits significantly higher computational costs with respect to the other algorithms. The derivative-free optimization methods achieve substantial improvements

in efficiency while maintaining comparable accuracy. In particular, Brent's Method and Nelder-Mead stand out for their rapid convergence, making them attractive candidates for large-scale empirical applications where repeated estimations are required. By contrast, GS, although conceptually simple and robust, quickly becomes computationally impractical as the grid step is refined.

## 5. Implementation and data analysis

Estimator (4) was employed to obtain static estimate of the parameter  $H$  using a six-market-year window of  $\nu = 1512$  observations of:

- the logarithm of the CBOE VIX Index, spanning from January 2, 1990, to September 17, 2025, for a total of 9,018 observations;
- the logarithm of 5-minute realized volatility of the S&P 500 (SPX), from January 3, 2000 to June 27, 2018, totaling 4,713 observations.

Estimator (24) was applied to the VIX and realized volatility series with parameters  $a = 1$ ,  $\bar{a} = 21$ , one-month market horizon, and a subsequence length  $T = \nu - \bar{a}$ , which entails a 95%-confidence interval of  $\hat{H}_0 \pm 0.1378$ .

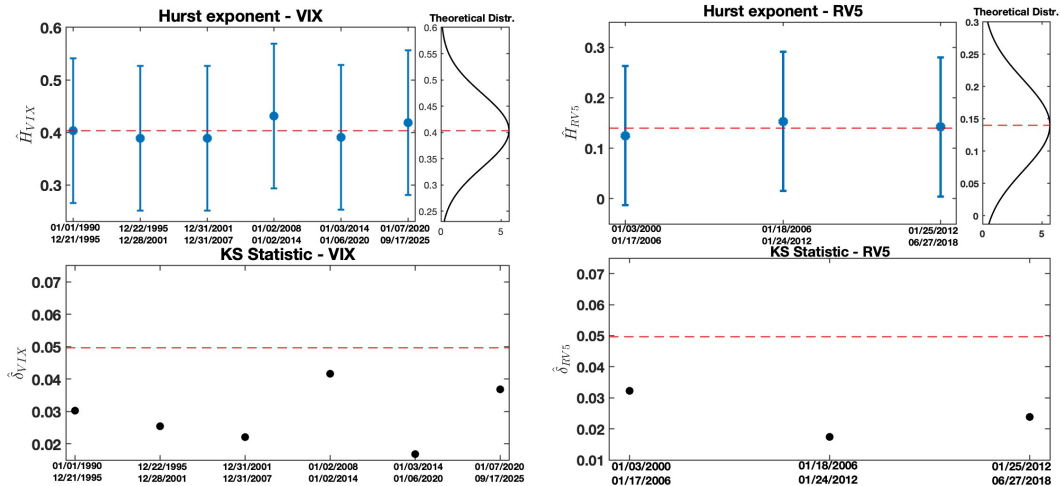


Figure 2: Estimates of the Hurst exponent  $\hat{H}$  (eq. (4)) and the Kolmogorov-Smirnov statistics  $\hat{\delta}$  (eq. (3)) for the VIX and 5-minute realized volatility (RV5). The top-left panel reports the estimates of  $\hat{H}_{VIX}$  with corresponding 95%-confidence intervals, while the top-right panel shows the analogous results for  $\hat{H}_{RV5}$ . The theoretical normal distributions used for comparison are displayed in the side of each panels (sample means are represented by red dashed lines). The bottom panels present the corresponding KS statistics  $\hat{\delta}_{VIX}$  and  $\hat{\delta}_{RV5}$ , together with the 5% critical value (red dashed line).

Figure 2 presents the results of the static analysis of the  $\hat{H}_0$  and KS statistics  $\hat{\delta}$  for the VIX and realized volatility. In the top-left panel, the  $\hat{H}_{VIX}$  is estimated over six equal, non-overlapping windows. Alongside, the theoretical normal distribution with mean equal to the sample average and variance given by (12). The 95%-confidence interval is  $\bar{\hat{H}}_{VIX} = 0.4039 \pm 0.1378$ . A  $\chi^2(5) = 0.4284$  test indicates that all estimates are drawn from the theoretical distribution, showing that  $\hat{H}_{VIX}$  remains constant over time. Overall, the results reinforce the conclusion that  $\hat{H}_{VIX}$  exhibits stability across different time frames and methodologies employed for analysis. The theoretical normal distribution has a 95%-confidence interval  $\bar{\hat{H}}_{RV5} = 0.1391 \pm 0.1378$ . In this case as well, a  $\chi^2(2) = 0.0721$  test suggests the stability of the realized volatility over time. In the bottom panels, the KS statistics are shown. For all estimates,  $\hat{\delta}$  lie below the 5% critical level  $K_{0.05} = 0.0497$ . All estimates are obtained using Brent's Method (BM). Therefore, we tested the null hypothesis  $H_0 : \bar{\hat{H}}_{VIX} = \bar{\hat{H}}_{RV5}$  against the one-sided alternative  $H_1 : \bar{\hat{H}}_{VIX} > \bar{\hat{H}}_{RV5}$ . The test statistic was  $z = 2.6636$ , yielding a one-sided p-value of 0.0037, thus providing strong evidence that the regularity of the VIX exceeds the regularity of realized volatility.

As documented also in previous studies, the values of  $\hat{H}_{VIX}$  are significantly higher than those obtained by applying the same method to the 5-min realized volatility. The values are in line with estimates in, e.g., [22, 21, 13] and many other studies. The difference in the value of  $\hat{H}$  between the VIX and the realized volatility is consistent with the findings in [28, 27], who examine the implied volatility-based approximations of the spot volatility. In particular, using at-the-money options on the S&P500 index with short maturity, [28] confirm roughness, but with a parameter of order 0.4, larger than that usually obtained from historical data (values less than 0.2), and explain the difference with the smoothing effect due to the remaining time to maturity of the considered options. The difference is reasonable and stems primarily from the nature of the VIX as a forward-looking measure derived from option prices, which inherently smooths short-term fluctuations through market expectations and averaging across strikes. In contrast, historical volatility is computed from high-frequency return data, capturing microstructure noise, jumps, and short-term market dynamics that contribute to a rougher appearance.

## 6. Conclusions

The core novelty of this work lies in the development and application of a distribution-based estimator that utilizes the Kolmogorov-Smirnov statistic to test the equality of

the distributions of rescaled log-volatility, rather than relying solely on scaling relationships of individual moments. This methodology captures richer structural information and is designed to be more robust against nonlinear biases that can affect moment-based estimators.

A central methodological innovation addresses the pronounced temporal dependence inherent in volatility. We introduce a random permutation procedure which, for sufficiently large permutation lengths, effectively decorrelates the data while preserving the marginal distribution of the increments (Proposition 2.5). This enables the valid application of the KS framework to dependent data, thereby facilitating rigorous statistical inference. Furthermore, we derive the asymptotic variance of the estimator (Proposition 2.6), providing a basis for constructing confidence intervals and assessing statistical significance. Specifically, we show that the estimator converges at the rate  $O_p(1/\sqrt{n} + 1/\sqrt{m})$ , where  $n$  and  $m$  denote the sizes of the rescaled sampling distributions.

From a computational standpoint, our analysis demonstrates that derivative-free optimization algorithms – particularly Brent’s method and the Nelder-Mead simplex – yield substantial efficiency gains, often by orders of magnitude, relative to a naive grid search, while preserving comparable estimation accuracy. This finding is crucial for enabling the application of the methodology to large-scale empirical studies and real-time analysis.

We apply the estimator to two central measures of market volatility: the VIX index and the 5-minute realized volatility of the S&P 500. We provide a theoretical justification that the regularity of the VIX is larger than that of the realized volatility (Propositions 3.1 and Remark 3.2), since the conditional expectation operator underlying the VIX, combined with integration over a future time horizon, inherently reduces variance and enhances regularity relative to the simple averaging used in realized volatility estimation. Consistently with this theoretical result, our empirical analysis indicates that the VIX exhibits a higher Hurst exponent ( $\hat{H}_{\text{VIX}} \approx 0.40$ ) than realized volatility ( $\hat{H}_{\text{RV}} \approx 0.14$ ), implying that implied volatility is substantially smoother. The fact that both implied and realized volatility display Hurst exponents significantly below 1/2 underscores a critical open problem in fractional modeling: the intrinsic coupling of roughness (a local property) and memory (a global, asymptotic property) in the Hurst parameter  $H$ . Our results highlight the necessity of developing models capable of disentangling these two features [9, 19].

**Acknowledgements & Funding.** This research was supported by Sapienza University of Rome under Grant No. RM120172B346C021.

## References

- [1] P. Abry, P. Gonçalves, and D. Veitch. Wavelet-based estimation of the self-similarity parameter of long-range dependent signals. *Statistical Methodology*, 6(1):33–52, 2009.
- [2] E. Alòs, J. A. León, and J. Vives. On the short-time behavior of the implied volatility for jump-diffusion models with stochastic volatility. *Finance and Stochastics*, 11(4):571–589, 2007.
- [3] T. G. Andersen, T. Bollerslev, F. X. Diebold, and P. Labys. Modeling and forecasting realized volatility. *Econometrica*, 71(2):579–625, 2003.
- [4] D. Angelini and S. Bianchi. Nonlinear biases in the roughness of a fractional stochastic regularity model. *Chaos, Solitons & Fractals*, 172:113550, 2023.
- [5] D. Angelini and S. Bianchi. Kolmogorov–Smirnov estimation of self-similarity in long-range dependent fractional processes. *Physica D: Nonlinear Phenomena*, 476:134697, 2025.
- [6] R. T. Baillie. Long memory processes and fractional integration in econometrics. *Journal of Econometrics*, 73(1):5–59, 1996.
- [7] R. T. Baillie, F. Calonaci, D. Cho, and S. Rho. Long memory, realized volatility and heterogeneous autoregressive models. *Journal of Time Series Analysis*, 40(4):609–628, 2019.
- [8] C. Bayer, B. Horvath, and A. Muguruza. Deep calibration of rough stochastic volatility models. *Quantitative Finance*, 21(1):25–41, 2021.
- [9] M. Bennedsen, A. Lunde, and M. S. Pakkanen. Decoupling the short- and long-term behavior of stochastic volatility. *Journal of Financial Econometrics*, 20(5):961–1006, 2022.
- [10] M. Bennedsen, M.S. Pakkanen, and A. Lunde. Learning the roughness of stochastic volatility from option prices. *Journal of Financial Econometrics*, 19(3):403–431, 2021.
- [11] S. Bianchi. A new distribution-based test of self-similarity. *Fractals*, 12(03):331–346, 2004.
- [12] S. Bianchi and D. Angelini. Fair volatility: A framework for reconceptualizing financial risk. *ArXiv preprint arXiv:2509.18837*, 2025.
- [13] G. Brandi and T. Di Matteo. Multiscaling and rough volatility: An empirical investigation. *International Review of Financial Analysis*, 84:102324, 2022.
- [14] R. Brent. *Algorithms for Minimization Without Derivatives*. Prentice-Hall, 1973.
- [15] J.-F. Coeurjolly. Simulation and identification of the fractional Brownian motion: A bibliographical and comparative study. *Journal of Statistical Software*, 5:1–53, 2000.
- [16] F. Comte and E. Renault. Long memory in continuous-time stochastic volatility models. *Mathematical Finance*, 8(4):291–323, 1998.
- [17] R. Cont. Empirical properties of asset returns: stylized facts and statistical issues. *Quantitative Finance*, 1(2):223–236, 2001.

- [18] Z. Ding, C. W. J. Granger, and R. F. Engle. A long memory property of stock market returns and a new model. *Journal of empirical finance*, 1(1):83–106, 1993.
- [19] I. Eliazar. Power Brownian motion. *Journal of Physics A: Mathematical and Theoretical*, 57(3):03LT01, dec 2023.
- [20] M. Fukasawa, T. Takabatake, and R. Westphal. Is volatility rough? *arXiv preprint arXiv:1905.04852*, 2019.
- [21] M. Fukasawa, T. Takabatake, and R. Westphal. Consistent estimation for fractional stochastic volatility model under high-frequency asymptotics. *Mathematical Finance*, 32(4):1086–1132, 2022.
- [22] J. Gatheral, T. Jaisson, and M. Rosenbaum. Volatility is rough. *Quantitative Finance*, 18(6):933–949, 2018.
- [23] D. E. Goldberg. *Genetic Algorithms in Search, Optimization, and Machine Learning*. Addison-Wesley, 1989.
- [24] R. Hooke and T. A. Jeeves. “Direct search” solution of numerical and statistical problems. *Journal of the ACM (JACM)*, 8(2):212–229, 1961.
- [25] S. Kirkpatrick, C. D. Gelatt Jr, and M. P. Vecchi. Optimization by simulated annealing. *Science*, 220(4598):671–680, 1983.
- [26] B. Lacaze and D. Roviras. Effect of random permutations applied to random sequences and related applications. *Signal Processing*, 82(6):821–831, 2002.
- [27] F. Le Floc'h. Roughness of the implied volatility, arxiv, 2207.04930, 2022.
- [28] G. Livieri, S. Mouti, A. Pallavicini, and M. Rosenbaum. Rough volatility: Evidence from option prices. *IISSE Transactions*, 50(9):767–776, 2018.
- [29] J. A. Nelder and R. Mead. A simplex method for function minimization. *The Computer Journal*, 7(4):308–313, 1965.
- [30] K. E. Parsopoulos and M. N. Vrahatis. Recent approaches to global optimization problems through particle swarm optimization. *Natural Computing*, 1(2):235–306, 2002.
- [31] S.-H. Poon and C. W. Granger. Forecasting volatility in financial markets: A review. *Journal of Economic Literature*, 41(2):478–539, 2003.
- [32] M. Rosenbaum and V. Morel. Estimation of roughness parameters: Application to rough volatility modeling. *Finance and Stochastics*, 23(2):501–533, 2019.
- [33] M. J. Sánchez-Granero, M. Fernández-Martínez, and J. E. Trinidad-Segovia. Introducing fractal dimension algorithms to calculate the Hurst exponent of financial time series. *The European Physical Journal B*, 85(86):1–13, 2012.
- [34] J. E. Trinidad-Segovia, M. Fernández-Martínez, and M. A. Sánchez-Granero. A note on geometric method-based procedures to calculate the Hurst exponent. *Physica A: Statistical Mechanics and its Applications*, 391(6):2209–2214, 2012.
- [35] F. Wei and R. M. Dudley. Two-sample Dvoretzky–Kiefer–Wolfowitz inequalities. *Statistics & Probability Letters*, 82(3):636–644, 2012.
- [36] A. T. A. Wood and G. Chan. Simulation of stationary Gaussian processes in  $[0, 1]^d$ . *Journal of Computational and Graphical Statistics*, 3(4):409–432, 1994.